Title

MR Thermometry during Transcranial MR Imaging-Guided Focused Ultrasound Procedures: A Review.

Permalink

https://escholarship.org/uc/item/4866m02q

Journal

American Journal of Neuroradiology, 45(1)

Authors

Mattay, Raghav

Kim, Kisoo

Shah, Lubdha

et al.

Publication Date

2023-12-29

DOI

10.3174/ajnr.A8038

Peer reviewed

MR Thermometry during Transcranial MR Imaging–Guided Focused Ultrasound Procedures: A Review

Raghav R. Mattay, Kisoo Kim, Lubdha Shah, Bhavya Shah, Leo Sugrue, Fatima Safoora, Eugene Ozhinsky, and Kazim H. Narsinh

ABSTRACT

SUMMARY: Interest in transcranial MR imaging–guided focused ultrasound procedures has recently grown. These incisionless procedures enable precise focal ablation of brain tissue using real-time monitoring by MR thermometry. This article will provide an updated review on clinically applicable technical underpinnings and considerations of proton resonance frequency MR thermometry, the most common clinically used MR thermometry sequence.

ABBREVIATIONS: CEM43 = cumulative equivalent minutes at 43°C; 2DFT = 2D Cartesian Fourier transform; GRE = gradient recalled-echo; HIFU = high-intensity focused ultrasound; LIFU = low-intensity focused ultrasound; MRgFUS = MR imaging–guided focused ultrasound; MRT = MR thermometry; NPV = nonperfused volume; PRF = proton resonance frequency

Transcranial MR imaging–guided focused ultrasound (MRgFUS) is an incisionless technique to precisely deliver energy through an intact skull for the treatment of a wide range of neurologic disorders, because the technique is minimally invasive and has a rapid recovery time.[1-4] MRgFUS is most commonly used to ablate brain tissue in a targeted fashion.[5] The FDA cleared MRgFUS for ablation of the ventralis intermediate nucleus of the thalamus to treat essential tremor in 2016[6] and, more recently, for the globus pallidus interna for treatment of advanced Parkinson disease.[7] Currently, the FDA-cleared system for transcranial MRgFUS is the ExAblate Neuro system (Insightec). The Insightec ExAblate Neuro system can be used with 2 different frequency transducers, referred to colloquially as high-intensity focused ultrasound (HIFU) and low-intensity focused ultrasound (LIFU). Operating at 650 kHz, the HIFU transducer enables precise ablation of brain tissue, while the LIFU transducer, operating low-intensity pulsed ultrasound at a frequency of 220 kHz, enables neuromodulation, BBB disruption, and acoustic activation of drug agents. Transcranial MRgFUS

systems have shown potential in clinical trials for treating trigeminal neuralgia (HIFU),[8] disrupting the BBB (LIFU),[9,10] activating sonodynamic therapy (LIFU),[11] or treating obsessive-compulsive disorders (LIFU).[12] Because HIFU causes thermal ablation, MR thermometry (MRT) is of the utmost importance. Depending on the clinical indication and location of the target, LIFU can be used with or without MRT. Laser interstitial therapy, a minimally invasive neurologic surgery using a laser on a probe, can also thermally ablate tissue, also requiring MRT for intraprocedural guidance.

Most of the current HIFU target structures are in the subcortical brain surrounded by critical fiber tracts.[13] In the treatment of essential tremor, the ventralis intermediate nucleus abuts the corticospinal tract laterally. Submillimetric errors in localization can result in complications such as gait imbalance or hemiplegia. The ventralis caudalis and medial lemniscus, located in proximity posteriorly, pose a potential risk of unintended heating that could lead to sensory abnormalities such as paresthesia, including the dreaded complication of anesthesia dolorosa (we will use the Hassler classification of thalamic nuclei for this article). HIFU ablation in the brain typically requires "align" (or "test") sonications to raise focal zone temperatures above 40°C and "verify" (or "stun") sonications to raise focal zone temperatures to approximately 50–52°C. The align sonications allow submillimetric triangulation and correction of the focal zone, while verify sonications produce a reversible physiologic effect allowing assessment of treatment response and adverse effects before the final ablative sonications that raise focal zone temperatures above 55°C. In general, with increasing temperatures, the exposure time needed to reach the ablation threshold drops exponentially. LIFU induces
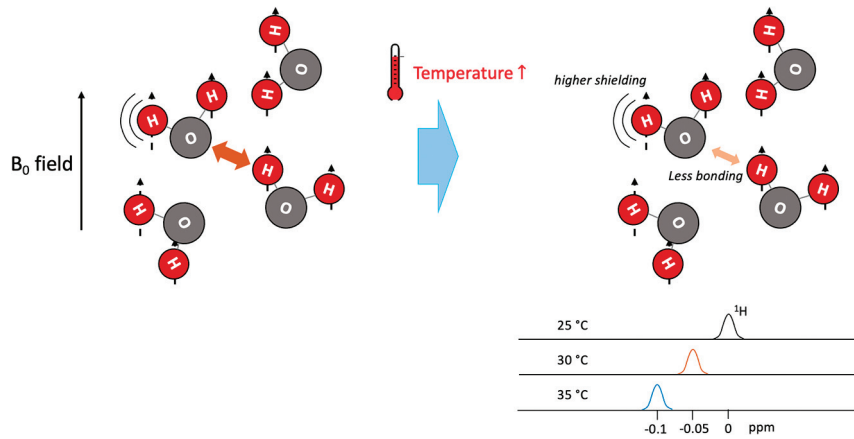
FIG 1. PRF is dependent on temperature. The B_0 field denotes the direction of the magnetic field and thus the spins of the hydrogen protons (H). An increase in temperature leads to less hydrogen bonding and higher electron shielding of protons, making them less susceptible to the B_0 field and decreasing their resonant frequency.

physiologic and biologic effects without an appreciable increase in temperature (eg, <0.1°C) within the target region, while avoiding tissue damage and microbleeding.[14] Real-time and noninvasive MRT is critical to achieve precise and controlled transcranial focused ultrasound treatments.

MRT comprises a set of thermal-sensitive MR imaging parameters, such as proton resonance frequency (PRF) shift, T1 and T2 relaxation times, diffusion, proton density, and magnetization transfer.[15] Some of these methodologies could be useful in nonaqueous tissues such as breast or bone but are less than optimal for clinical intracranial applications because they often require longer acquisition times to obtain an adequate SNR. A recent review discusses MRT in cerebrovascular disease as a versatile tool for diagnosis, prognostication, and monitoring treatment response.[16] For MRgFUS, PRF thermometry is the mainstay for current clinical applications due to fast acquisition times and high temperature sensitivity within aqueous tissues. Several factors can influence the optimal measurement of temperature change in the target tissue using PRF, including heterogeneous heat deposition at the focal zone, tissue properties, tissue inhomogeneity, the presence of increased susceptibility, timing of the acquisition, and motion artifacts. The consideration of these factors is imperative to ensure the successful implementation of transcranial MRgFUS applications.

This review aims to provide a basic introduction to PRF thermometry and to discuss factors that influence temperature measurements in transcranial MRgFUS applications for both physicians and scientists wishing to further develop the safety and efficacy of this exciting emerging technology.

PRF Thermometry

Within the B_0 magnetic field, hydrogen protons in water and fat precess around their axis at their resonant frequencies according to their gyromagnetic ratio. Temperature variations in tissue cause changes in the angular frequency of the proton precession. For hydrogen nuclei, which comprise a single proton, temperature effects result in frequency shifts less than a few 100 Hz at 1.5T, but

they remain detectable (for comparison, the resonance frequency of a proton at 1.5T is 63.87 MHz).

The electron cloud of a hydrogen atom intrinsically shields the proton within the nucleus from the surrounding magnetic field. While hydrogen atoms in individual water molecules are strongly linked through covalent bonds to their associated oxygen atoms, they also experience weaker attraction to the oxygen atoms of neighboring water molecules through hydrogen bonding. Hydrogen bonding causes some of the electron clouds of hydrogen to be pulled away by the electrophilic oxygen atom, resulting in deshielding the hydrogen protons. With this deshielding, protons within water molecules experience a stronger local magnetic field. The local magnetic field can be addressed as follows:

Equation 1 $$B_{loc}(T) = (1 - s(T) + \chi(T)B_0,$$

Equation 2 $$s(T) = \alpha T,$$

where T is a temperature, $s(T)$ is the shielding constant of water molecules, $\chi(T)$ is the magnetic susceptibility of tissue, B_0 is the strength of the main MR imaging magnetic field, and α is the temperature coefficient of the water proton, approximately 0.01 ppm/°C (the coefficient ranges from -0.00739 to -0.0135 ppm/°C).[17,18]

Increasing the temperature of tissue disrupts hydrogen bonding within water molecules, improving the shielding of hydrogen protons. In contrast, in aqueous tissues, the temperature-dependent magnetic susceptibility of tissue $\chi(T)$ can be negligible because it is much smaller than effects due to changes in the shielding of hydrogen protons.

Equation 3 $$\omega(T) = \gamma B_{loc}(T),$$

where ω is the Larmor angular frequency and γ is the gyromagnetic ratio of the hydrogen nuclei (267.522×10^6 rad/s/T). Hydrogen nuclei in water at higher temperatures have lower corresponding resonant frequencies due to decreased hydrogen bonding (Fig 1). PRF thermometry relies on these changes in resonance frequency in hydrogen nuclei within water[17] in response to local changes in tissue temperature. For example, in a 1.5T magnetic field, an increase of 1°C would result in a decrease in the PRF of 0.6387 Hz.[19] Hence, temperature changes result in local resonant frequency variations. The measured temperature change is relative and is based on the assumption that the reference body temperature is 37°C.

There are several methods to estimate the temperature using the relationship between water proton frequency and temperature. MRS imaging provides the nuclear magnetic resonance signal spectrum, allowing monitoring the frequency peak of the water proton.
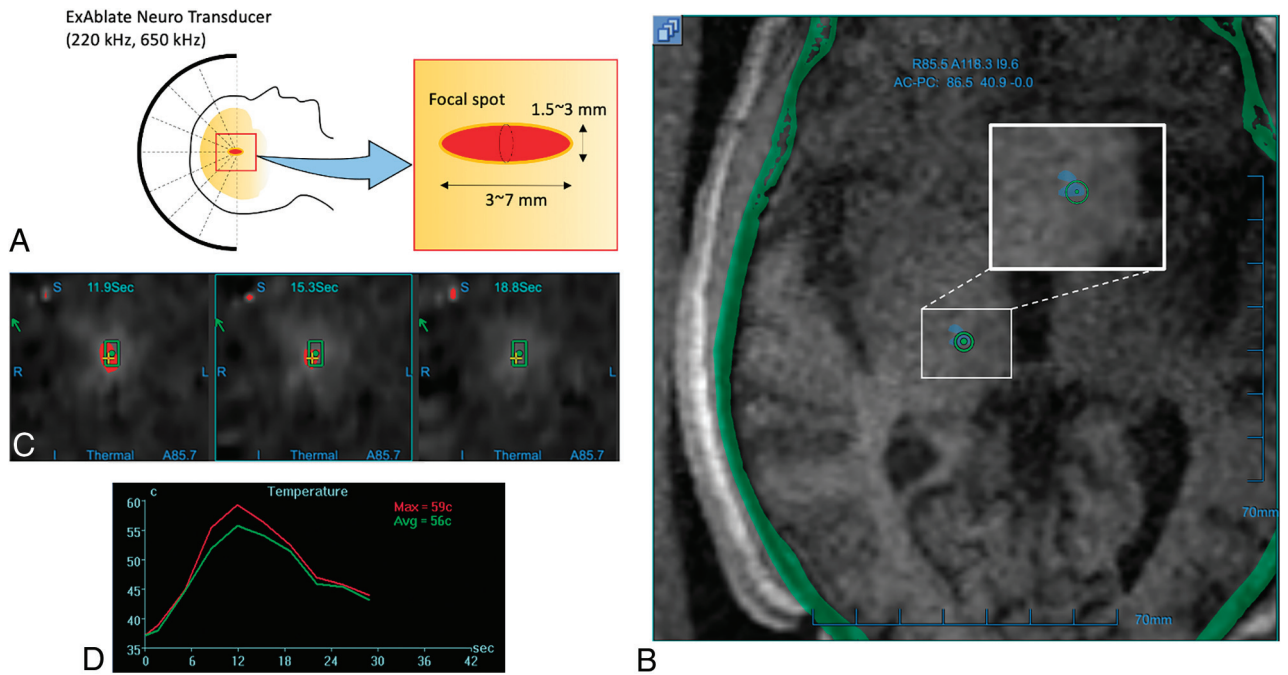
FIG 2. MR imaging thermometry during transcranial focused ultrasound. *A*, The focal spot of the ExAblate Neuro transducer takes a prolate ellipsoid shape, measuring approximately 1.5 mm in diameter and 3 mm in length at 650 kHz and approximately 3 mm in diameter and 7 mm in length at 220 kHz. *B*, The PRF thermal dose map shows an accumulated thermal dose in light blue, which is based on the CEM43 model. The thermal dose map visualizes the amount of heat deposited into the target tissue, allowing clinicians to optimize treatment parameters and positioning while minimizing the risk of normal tissue damage. *C*, Multiple MRT images are obtained during sonication. In this example, images are acquired at 11.9 seconds (*left panel*), 15.3 seconds (*middle panel*), and 18.8 seconds (*right panel*) after the sonication has begun, generating images of tissue temperature at the focal spot according to a user-determined color scale. The time intervals between images will vary depending on the user-determined settings, such as the addition of presonication baseline phases or changing from multiple- to single-echo thermometry. The duration of the sonication is often set so that peak temperatures are achieved in sync with the MRT acquisition. The alignment of the focal spot to the target is best assessed in the phase-encoding direction. *D*, After sonication, a temperature graph is generated to show average and maximal temperatures across time within the ROI. Avg indicates average; Max, maximum.

On the basis of spectroscopic imaging, the temperature can be estimated by observing the frequency difference between the water proton and the reference, such as the tissue lipid[20] or contrast agents.[21] PRF-based MRS imaging is the sole method capable of measuring absolute temperature with high accuracy (eg, 0.3°C for 1-mL voxels[22]). Nevertheless, most MRS techniques are limited in terms of spatial resolution and real-time MR imaging acquisition, which are necessary for rapid temperature monitoring in transcranial MRgFUS applications. The other approach is to use MR phase mapping because changes in the temperature can alter the MR resonance frequency. In phase mapping–based PRF thermometry, temperature-induced local frequency variations can be detected using spoiled gradient recalled-echo (GRE) sequences to acquire phase maps before and during tissue heating. By subtracting the baseline phase images from the subsequent phase images acquired during heating, chemical shift effects that are not temperature-dependent are theoretically removed. Phase differences caused by field deviations within biologic tissues can be used for estimating relative changes in temperature as follows:

$$\text{Equation 4} \qquad \Delta T = \frac{\phi(T) - \phi(T_0)}{\gamma \alpha B_0 TE},$$

where ΔT is the temperature difference relative to the reference image, $\phi(T)$ is the current phase image, $\phi(T_0)$ is the reference phase image, γ is the gyromagnetic ratio, α is the temperature-sensitive coefficient, B_0 is the main magnetic field, and TE is the echo time. The reference phase image (before heating) is subtracted from the current phase image (during heating). Finally, relative changes in temperature can be calculated.

PRF thermometry allows temperature maps to be acquired in seconds,[15] noting that it has suboptimal performance in adipose tissue, making it less ideal for body applications of HIFU but appropriate for transcranial HIFU. Because HIFU generally creates a focal spot in a prolate ellipsoid shape that is 3–4 mm in diameter and 4–5 mm in height[23] (Fig 2), the PRF sequence resolution must have an in-plane resolution of at least 1–2 mm and a section thickness maximum of 3 mm.[24] In general, clinical imaging systems have a temperature precision of approximately 1°–2°C[25] and are typically acquired during ablation,[26] with the most important image acquired after the sonication peak. Specifically, for the transcranial HIFU Insightec ExAblate Neuro system using a body coil for receive and transmit and a gradient-echo sequence (FOV = 280 mm; frequency = 256; phase = 128; section thickness = 3mm; matrix = 256 × 256), the spatial resolution is 1.09 × 1.09 × 3 mm and the temporal resolution is ~3.5 seconds per dynamic image with a total acquisition of <1 minute for each sonication. Currently a standard diagnostic head imaging coil cannot be used with the Insightec ExAblate Neuro device. Also, current MRT used for
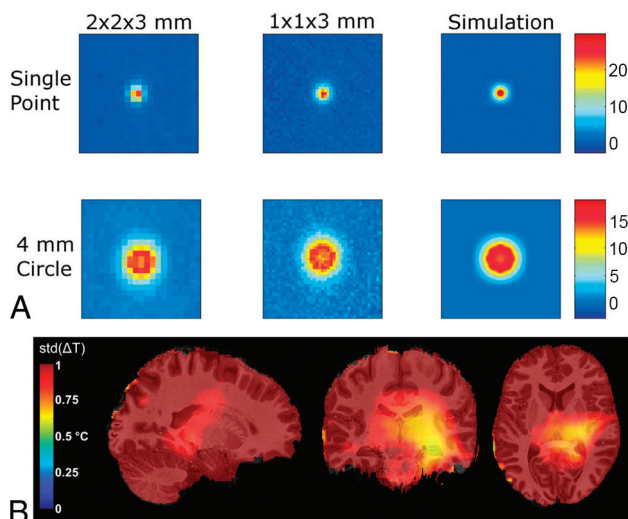
FIG 3. Sources of error in MR imaging thermometry. *A*, Temperature maps during HIFU heating using different spatial resolutions (left to right: $2 \times 2 \times 3$ mm³, $1 \times 1 \times 3$ mm³, $0.1 \times 0.1 \times 0.1$ mm³ simulation). This experiment showed that imaging with a spatial resolution of $1.0 \times 1.0 \times 3.0$ mm³ or higher with slices oriented perpendicular to the beam path resulted in the best accuracy of temperature measurement (figure reproduced from Todd et al[24] with permission). *B*, Temporal SD (std) of PRF temperature maps overlaid on sagittal, coronal, and axial MR images demonstrate errors in temperature measurement due to motion (eg, B_0 field drift, cardiac pulsation, respiratory motion; figure reproduced from Le Ster[75]).

transcranial HIFU with Insightec equipment can only be acquired in 2 dimensions and must be acquired in 1 of 3 orthogonal planes during sonication.

Thermal Dosimetry

Dosimetry models are used to estimate thermal tissue damage during HIFU procedures. When the PRF temperature map is obtained, the cumulative equivalent minutes at 43°C (CEM43) model can be used to estimate a thermal isoeffect dose through the exposure time.[27,28]

Equation 5
$$CEM43 = \int_0^t R^{(43-T)} dt,$$

where R is the factor depending on temperature range: 0.25 (T ≤ 43°C) and 0.5 (T > 43°C). van Rhoon et al[28] reported the challenges in establishing precise thermal thresholds for brain tissue due to the substantial differences in species, data availability, and a lack of such data in humans. However, previous investigations reported that thermal tissue damage can occur in the range of 10 CEM43, and a thermal dose as low as 0.1 CEM43 can result in changes in the BBB permeability, metabolism, CBF, and neural activity.[29] Hence, close monitoring and careful control of the thermal dose are especially helpful to ensure the safety and efficacy of transcranial HIFU (Fig 2B). Of note, when performing LIFU for neuromodulation in neuropsychiatric diseases, it is recommended to keep the thermal dose below 0.1 CEM43 to minimize uncontrolled physiologic changes. Thus, depending on the clinical indication and target, thermometry is often not used for LIFU.

Optimization of PRF Thermometry

Trade-Offs. As in other MR imaging, in PRF thermometry there are trade-offs among spatial resolution, temporal resolution, and SNR. Todd et al[24] showed that the spatial resolution needed to capture nonuniform temperature distributions created by HIFU (Fig 3A) is highly dependent on the shape of temperature distribution. Low-resolution imaging was sufficient in accurate measurement of a temperature distribution that changes linearly in space. However, higher spatial resolution is needed when the temperature distribution is nonlinear, which is often the case in HIFU, in which the distribution is based on the shape and size of the focal zone, the heating trajectory, and the ultrasound power and deposition. Their experiments showed that imaging with a spatial resolution of $1.0 \times 1.0 \times 3.0$ mm³ or higher with slices oriented perpendicular to beam path resulted in the best accuracy of temperature measurement. Because the HIFU thermal ablation lesion at the focal zone is elongated in the craniocaudal direction (as a prolate ellipsoid), there is inherently less curvature of the temperature distribution in the direction of the beam, allowing thicker acquisition slices to be used. Thus, PRF thermometry is often acquired in the axial plane because small errors in section prescription on coronal or sagittal imaging may result in missing the hot spot.

Image SNR

The phase-dependent SNR from these images is proportional to the PRF change as well as the sequence TE.[15] As shown in Equation 2, when the T2* relaxation time of brain tissues is equal to the TE, the optimal SNR can be achieved.

Equation 6
$$SNR \propto TEe^{-\frac{TE}{T_2^*}}.$$

To perform MRT that has sensitivity on the order of 0.01 ppm, a high degree of magnetic field homogeneity is required. In standard 2D Cartesian Fourier transform (2DFT) thermometry, when all available time in a TR is used for sampling to maximize the SNR, the result is a long imaging time, which makes the images more sensitive to off-resonance/local frequency change.

Magnetic Field Inhomogeneity

Magnetic field inhomogeneity can be conceptualized in terms of external magnetic flux and local magnetic susceptibility. These sources of error include magnetic field drift and susceptibility changes.[31,32] Magnetic field drift refers to the change in the magnetic field flux due to extrinsic factors such as the flux in the earth's own magnetic field and gradient system heating that occurs when applying large gradients.[32] Magnetic field phase drifts in clinical scanners while scanning have been reported to be from 0.01 to 0.06 ppm/min (or 0.6×3.6 ppm/h), which could result in up to approximately 6°C/min of scan time (assuming a PRF coefficient of -0.008 ppm/°C).[33] Depending on the polarity, these field drifts can result in both over- and underestimation.[34] Because the drift is small during acquisition, it can be corrected with postprocessing using internal or external references such as aqueous tissue outside the heating zone (as in referenceless thermometry described below) or fat-based tissues (with minimal phase shift due to heat).[35]

Susceptibility changes due to inhomogeneity in a patient's tissues can also greatly affect temperature measurement. Briefly, susceptibility is caused by paramagnetic, ferromagnetic, or diamagnetic substances (ie, Ca^{2+}) and is particularly noticed at the interface of 2 different substances (eg, between gas and bone).[36] Blood flow parameters also greatly affect magnetic inhomogeneity, such as deoxyhemoglobin concentration, blood flow, hematocrit, red blood cell integrity, and vessel orientation. Additionally, other relevant factors that affect homogeneity include molecular diffusion, pH, and prior contrast use.[37]

Off-Resonance Sensitivity
The multiecho approach is an effective method for mitigating off-resonance sensitivity while maintaining SNR. In early multiecho 2DFT sequences, temperature was estimated by determining the slope of the linear fit of the phase versus TEs.[38] While multiecho sequences were of similar scan length to those of single-echo gradient images with long TEs, they allowed less aliasing/phase wrapping (ie, the ability to detect temperature increases of ≥100°C). The multiecho approach compared with the single-echo gradient approach showed less aliasing at sites of bone and fat as well.[38] Furthermore, the multiecho images showed less degradation from motion and greater ability to identify areas with multiple spectral components. Newer approaches combining multiple independent temperature estimates can be performed to optimize temperature SNR.[39,40]

Electrical Properties
Temperature change in ablated tissue can also lead to change in the electrical properties of the tissue, causing a constant incremental phase shift per unit change in temperature completely independent of the TE.[41] Increasing temperature leads to an increase in electrical conductivity, causing more attenuation in the amplitude of the MR radiofrequency pulses used for imaging acquisition, affecting the phase and ultimately temperature measurement. This typically affects procedures that heat larger tissue volumes like deep regional hyperthermia and is less consequential in ablative procedures like MRgFUS, in which the ablation zone is smaller and much more focused.

Spatial Sampling: Frequency versus Phase-Encoding Direction
Chemical shift artifacts are noted on spin-echo anatomic imaging at the interface between fat and water due to slightly different resonant frequencies of hydrogen nuclei within lipid and water (because there is no deshielding of the hydrogen nuclei in lipid). These cause a spatial misregistration of the fat and water molecules in the frequency-encoding direction. For standard gradient-echo sequences and PRF thermometry, the sensitivity of these distortions is larger in the frequency-encoding than in the phase-encoding direction.[42] This phenomenon should be considered when performing geometric adjustments in the ExAblate Neuro system. If a focal spot is generated with an offset between the current and planned spot location, the system allows electronic adjustments to the focal spot. In this process, the frequency direction can be ignored because MR images may display shifted geometric information, making it unnecessary to consider the frequency-encoding direction during the adjustment procedure. Thus, intraoperative thermal measurements only in the phase-encoding direction are recommended (Fig 2C).

Motion Sensitivity
Current clinical MRT sequences typically use a single baseline to reconstruct temperature maps so that a single preheating acquisition is subtracted from a postheating acquisition. This feature has been shown to work well in phantoms and stationery tissues but is susceptible to substantial artifacts when motion occurs. Currently, the Insightec ExAblate Neuro system performs a motion-detection scan in which areas of high contrast (eg, interface between pia mater/ependyma and CSF) are monitored during treatment. If motion is detected, sonication is aborted.

Motion leads to phase errors in the PRF calculation in various ways (Fig 3B). First, voxel-by-voxel phase subtraction results in a significant temperature error if there is image misregistration. Second, susceptibility changes of the magnetic field result in an additional phase value in the PRF calculation. Third, organ movement during MR image acquisition generates blurring and ghost artifacts, which may cause temperature bias or uncertainty, even if those artifacts may not directly affect PRF temperature maps. While more important in body clinical applications of HIFU due to the presence of respiratory motion, cardiac motion, and gut peristalsis, motion also degrades intracranial MRT, especially when considering that thermal ablative lesions in the thalamus require submillimetric precision to avoid complications. Head motion, brain pulsation (due to the effect of the cardiac cycle on cerebral perfusion[43] and CSF flow[44]), and facial motion (of the eyelids, tongue, pharynx, or jaw)[25,45] can all lead to aliasing artifacts and reduced SNR in single baseline imaging.

There are multiple additional methods to acquire thermometry, avoiding single baseline artifacts due to periodic and non-periodic motion, including multibaseline subtraction[46-48] and referenceless[49-51] and hybrid multibaseline/referenceless thermometry.[52] In multibaseline subtraction, a whole set of baseline images before heating is acquired over the entire respiratory and/or cardiac cycle to create a library. After heating, either the best baseline image of the library or an averaged composite image is used for baseline subtraction[46,53] In referenceless reconstruction, the baseline image is not used, but instead the temperature increase in every image is used. This is performed by estimating the background phase outside the heated region by fitting an equation/polynomial to the phase (ie, phase-regression analysis). This polynomial is then extrapolated to the location of heating, and a phase is estimated, which replaces the traditional baseline phase when calculated for phase shift and temperature. With this technique, there is a complete elimination of misregistration of images with the baseline data due to frame-to-frame motion.[50] However, the background phase at tissue interfaces requires larger polynomial orders to fit in referenceless reconstruction, potentially increasing the risk of underestimating the thermal dose.

In intracranial applications of MRgFUS, it is important to have whole-brain coverage, because it is important for monitoring potential heating of tissue in the near and far field of the ultrasound beam. However, it is difficult to apply a low-order

polynomial to the whole brain, especially in the frontal region and structures at the base of the brain that are adjacent to air-filled sinuses and nasal cavities.[25] A hybrid reconstruction combining both multibaseline and referenceless acquisitions was described in detail by Grissom et al[52] and is reported to be more robust to both motion-related artifacts and varying anatomic configurations in moving organs (liver and heart).

Rieke et al[25] compared absolute temperature error and temporal temperature uncertainty of different reconstruction techniques: single baseline subtraction, multibaseline subtraction (with 30 library images), hybrid single baseline/referenceless reconstruction, and hybrid multibaseline/referenceless reconstruction. In patients undergoing transcranial MRgFUS, hybrid reconstruction yielded only approximately 5% of pixels with >1°C of error. Hybrid multibaseline/referenceless reconstruction showed little improvement compared with multibaseline subtraction in the cases in which volunteers were instructed to be as still as possible; however, it substantially outperformed traditional multibaseline reconstruction when nonrepetitive motion was present (tongue or jaw motion). While hybrid multibaseline/referenceless reconstruction achieves the best results, it requires a longer time to acquire. A hybrid single-baseline/referenceless reconstruction can substantially reduce temperature errors and is adequate for measuring temperature within the central brain for the currently FDA-approved indications for transcranial MRgFUS (essential tremor and Parkinson disease), targeting nuclei within the thalamus and globus pallidus.

Recent technical developments for motion-robust MRT have been proposed, such as principal component analysis,[54] background field removal methods,[55] motion correction using machine learning,[56] and *k*-space-based methods.[57] However, most techniques have inherent trade-offs among spatial coverage, computational costs, and the accuracy of temperature measurement.

Coil Use
During transcranial MRgFUS, ultrasound hardware surrounds the head, occupying the space typically occupied by an MR imaging head coil during diagnostic imaging. Therefore, large-diameter coils such as a body coil are used for MRT acquisition currently, but these yield markedly lower SNR. Body coils are single-channel; therefore, techniques that use multiple receiver channels such as parallel imaging cannot be currently used.[58] Recently, a 2-channel receive-only head coil was designed specifically for use in conjunction with the ExAblate Neuro system and is being offered by Insightec to be used with 3T scanners.[59] Unlike a standard head coil, this coil is made integral with the membranes used in the Insightec machine and is disposable. As reported, the head coil improved the SNR on T2-weighted images compared with the volume body coil by 3–4 times. A higher SNR may have the potential to provide better treatment-planning, more precise temperature measurements, and ultimately better clinical results. Development of MRgFUS-compatible coil arrays that allow parallel imaging is a burgeoning area of research, because the currently developed MRgFUS coil arrays still have fewer coils than those used in conventional anatomic or functional parallel imaging (11 versus 32).[60]

Large-Brain-Volume MRT
Typically, PRF MRT is acquired using a spoiled GRE sequence in which temperature-induced local frequency variations lead to phase changes in the MR signal. As previously mentioned, the temperature sensitivity is maximized when the TE is the same as or closest to the T2* relaxation time within tissues. This required TE naturally leads to a longer TR in the GRE sequence, leading to extended total acquisition times and increased susceptibility to motion. Hence, acceleration strategies should be considered to improve the temporal resolution when measuring temperature over a large brain volume.

The Insightec ExAblate Neuro system offers 2 options for image acquisition: a single-section acquisition using a 2DFT GRE sequence or multisection acquisition (typically 3–5 slices) using EPI. While EPI can cover multiple slices, it is often associated with a lower SNR and susceptibility artifacts, which can cause spatial shifts in the resulting images. Other acceleration approaches include spiral and radial readout trajectories, as well as compressed sensing.[61-63] Recently, there has been growing interest in using accelerated imaging techniques to measure temperature over a large brain volume.[64]

Future Considerations
Beam Localization without MRT. The MR acoustic radiation force imaging technique is an emerging method that allows one to image the location of the focal spot without a small temperature rise.[65,66] A long sonographic impulse (1–20 ms) produces an acoustic radiation force that can create tissue displacements locally led by shear wave propagation. This displacement can be encoded in the phase direction of the MR image using bipolar motion-sensitizing gradients.[66] This step enables accurate spot localization, evaluation, calibration, and refocusing of the ultrasound focal zone without the test sonication that causes a small temperature rise.

MR Imaging Assessment of Treatment Outcomes
After MRgFUS treatment, the criterion standard assessment of the ablation zone is to measure nonperfused volume (NPV) using gadolinium-based contrast-enhanced MR imaging. After gadolinium injection, the region without enhancement characterizes the NPV, which is associated with the coagulated tissue.[67,68] However, intraprocedural postcontrast NPV assessment is generally not performed due to safety concerns regarding heating of the contrast as well as potential errors of MRT.[69-71] In clinical practice, DWI is obtained postprocedurally to estimate the ablation zone.

Alternatively, the cumulative thermal dose can offer important information for tissue response in HIFU treatment. In MRgFUS treatments for essential tremor, Huang et al[72] demonstrated that an accumulated thermal dose in the range of 17–240 CEM43 is highly correlated with lesion size measured by T1- and T2-weighted MR images. This finding may suggest that the cumulative thermal dose can help clinicians determine treatment end points in the procedure.

Multiple additional MR imaging methods are being developed and evaluated to detect treatment effects after MRgFUS, including T1/T2 mapping, magnetization transfer ratio, amide proton transfer, and MR elastography.[70,73,74] A combination of emerging

multiparametric MR imaging techniques may be needed to obtain a more comprehensive evaluation of tissue-level changes during and after MRgFUS.

CONCLUSIONS

As enthusiasm for incisionless transcranial MRgFUS continues to grow for a continually expanding set of indications; work to optimize reconstruction methods, mitigate common artifacts, and create dedicated coils will further improve PRF MRT for clinical use. An in-depth understanding of the MRT sequences, including pitfalls and limitations, will enable avoidance of complications during MRgFUS procedures by using real-time image guidance.

Disclosure forms provided by the authors are available with the full text and PDF of this article at www.ajnr.org.

REFERENCES

1. Meng Y, Hynynen K, Lipsman N. **Applications of focused ultrasound in the brain: from thermoablation to drug delivery.** *Nat Rev Neurol* 2021;17:7–22 CrossRef Medline
2. Abrahao A, Meng Y, Llinas M, et al. **First-in-human trial of blood–brain barrier opening in amyotrophic lateral sclerosis using MR-guided focused ultrasound**. *Nat Commun* 2019;10:4373 CrossRef Medline
3. Nicodemus NE, Becerra S, Kuhn TP, et al. **Focused transcranial ultrasound for treatment of neurodegenerative dementia.** *Alzheimers Dement (N Y)* 2019;5:374–81 CrossRef Medline
4. Chen SG, Tsai CH, Lin CJ, et al. **Transcranial focused ultrasound pulsation suppresses pentylenetetrazol induced epilepsy in vivo.** *Brain Stimul* 2020;13:35–46 CrossRef Medline
5. Dai H, Chen F, Yan S, et al. **In vitro and in vivo investigation of high-intensity focused ultrasound (HIFU) hat-type ablation mode.** *Med Sci Monit* 2017;23:3373–82 CrossRef Medline
6. **Premarket Approval (PMA).** https://www.accessdata.fda.gov/scripts/cdrh/cfdocs/cfPMA/pma.cfm. Accessed December 20, 2022
7. FDA. **Exablate Model 4000 Type 1.0 and 1.1 System ("Exablate Neuro")–P150038/S014.** January 3, 2022. https://www.fda.gov/medical-devices/recently-approved-devices/exablate-model-4000-type-10-and-11-system-exablate-neuro-p150038s014. Accessed December 20, 2022
8. Gandhi D. **MR Guided Focused Ultrasound (FUS) for the Treatment of Trigeminal Neuralgia.** 2022. https://clinicaltrials.gov/ct2/show/NCT04579692. Accessed December 19, 2022
9. Gandhi K, Barzegar-Fallah A, Banstola A, et al. **Ultrasound-mediated blood–brain barrier disruption for drug delivery: a systematic review of protocols, efficacy, and safety outcomes from preclinical and clinical studies.** *Pharmaceutics* 2022;14:833 CrossRef Medline
10. InSightec. **Blood-brain Barrier (BBB) Disruption Using Exablate Focused Ultrasound With Standard of Care Treatment of NSCLC Brain Mets.** 2022. https://clinicaltrials.gov/ct2/show/NCT05317858. Accessed December 19, 2022
11. Bunevicius A, Pikis S, Padilla F, et al. **Sonodynamic therapy for gliomas.** *J Neurooncol* 2022;156:1–10 CrossRef Medline
12. Goodman W. **Imaging-Guided Low Intensity Focused Ultrasound (LIFU) (LIFU).** 2022. https://classic.clinicaltrials.gov/ct2/show/NCT05467085. Accessed October 20, 2022
13. Feltrin FS, Chopra R, Pouratian N, et al. **Focused ultrasound using a novel targeting method four-tract tractography for magnetic resonance-guided high-intensity focused ultrasound targeting.** *Brain Commun* 2022;4:fcac273 CrossRef Medline
14. Baek H, Pahk KJ, Kim H. **A review of low-intensity focused ultrasound for neuromodulation.** *Biomed Eng Lett* 2017;7:135–42 CrossRef Medline
15. Rieke V, Butts Pauly K. **MR thermometry.** *J Magn Reson Imaging* 2008;27:376–90 CrossRef Medline
16. Dehkharghani S, Qiu D. **MR thermometry in cerebrovascular disease: physiologic basis, hemodynamic dependence, and a new frontier in stroke imaging.** *AJNR Am J Neuroradiol* 2020;41:555–65 CrossRef Medline
17. Ishihara Y, Calderon A, Watanabe H, et al. **A precise and fast temperature mapping using water proton chemical shift.** *Magn Reson Med* 1995;34:814–23 CrossRef Medline
18. Kuroda K. **Non-invasive MR thermography using the water proton chemical shift.** *Int J Hyperthermia* 2005;21:547–60 CrossRef Medline
19. Lewa CJ, de Certaines JD. **Body temperature mapping by magnetic resonance imaging.** *Spectrosc Lett* 1994;27:1369–419 CrossRef
20. Kuroda K, Mulkern RV, Oshio K, et al. **Temperature mapping using the water proton chemical shift: self-referenced method with echo-planar spectroscopic imaging.** *Magn Reson Med* 2000;43:220–25 CrossRef Medline
21. Lindner LH, Reinl HM, Schlemmer M, et al. **Paramagnetic thermosensitive liposomes for MR-thermometry.** *Int J Hyperthermia* 2005;21:575–88 CrossRef Medline
22. Marshall I, Karaszewski B, Wardlaw JM, et al. **Measurement of regional brain temperature using proton spectroscopic imaging: validation and application to acute ischemic stroke.** *Magn Reson Imaging* 2006;24:699–706 CrossRef Medline
23. Jeanmonod D, Werner B, Morel A, et al. **Transcranial magnetic resonance imaging-guided focused ultrasound: noninvasive central lateral thalamotomy for chronic neuropathic pain.** *Neurosurg Focus* 2012;32:E1 CrossRef Medline
24. Todd N, Vyas U, de Bever J, et al. **The effects of spatial sampling choices on MR temperature measurements.** *Magn Reson Med* 2011;65:515–21 CrossRef Medline
25. Rieke V, Instrella R, Rosenberg J, et al. **Comparison of temperature processing methods for monitoring focused ultrasound ablation in the brain.** *J Magn Reson Imaging* 2013;38:1462–71 CrossRef Medline
26. Kim YS, Trillaud H, Rhim H, et al. **MR thermometry analysis of sonication accuracy and safety margin of volumetric MR imaging-guided high-intensity focused ultrasound ablation of symptomatic uterine fibroids.** *Radiology* 2012;265:627–37 CrossRef Medline
27. Sapareto SA, Dewey WC. **Thermal dose determination in cancer therapy.** *Int J Radiat Oncol Biol Phys* 1984;10:787–800 CrossRef Medline
28. van Rhoon GC, Samaras T, Yarmolenko PS, et al. **CEM43°C thermal dose thresholds: a potential guide for magnetic resonance radiofrequency exposure levels?** *Eur Radiol* 2013;23:2215–27 CrossRef Medline
29. Yarmolenko PS, Moon EJ, Landon C, et al. **Thresholds for thermal damage to normal tissues: an update.** *Int J Hyperthermia* 2011;27:320–43 CrossRef Medline
30. Schmidt R, Frydman L. **Alleviating artifacts in 1H MRI thermometry by single scan spatiotemporal encoding.** *MAGMA* 2013;26:477–90 CrossRef Medline
31. Marx M, Pauly KB. **Improved MRI thermometry with multiple-echo spirals.** *Magn Reson Med* 2016;76:747–56 CrossRef Medline
32. El-Sharkawy AM, Schär M, Bottomley PA, et al. **Monitoring and correcting spatio-temporal variations of the MR scanner's static magnetic field.** *MAGMA* 2006;19:223–36 CrossRef Medline
33. Odéen H, Parker DL. **Magnetic resonance thermometry and its biological applications: physical principles and practical considerations**. *Prog Nucl Magn Reson Spectrosc* 2019;110:34–61 CrossRef Medline
34. De Poorter J, De Wagter C, De Deene Y, et al. **Noninvasive MRI thermometry with the proton resonance frequency (PRF) method: in vivo results in human muscle.** *Magn Reson Med* 1995;33:74–81 CrossRef Medline
35. Hofstetter LW, Yeo DT, Dixon WT, et al. **Fat-referenced MR thermometry in the breast and prostate using IDEAL.** *J Magn Reson Imaging* 2012;36:722–32 CrossRef Medline
36. Haacke EM, Xu Y, Cheng YCN, et al. **Susceptibility weighted imaging (SWI).** *Magn Reson Med* 2004;52:612–18 CrossRef Medline
37. Hermier M, Nighoghossian N. **Contribution of susceptibility-weighted imaging to acute stroke assessment.** *Stroke* 2004;35:1989–94 CrossRef Medline

38. Mulkern RV, Panych LP, McDannold NJ, et al. **Tissue temperature monitoring with multiple gradient-echo imaging sequences.** *J Magn Reson Imaging* 1998;8:493–502 CrossRef Medline

39. Madore B, Panych LP, Mei CS, et al. **Multipathway sequences for MR thermometry.** *Magn Reson Med* 2011;66:658–68 CrossRef Medline

40. Todd N, Diakite M, Payne A, et al. **In vivo evaluation of multi-echo hybrid PRF/T1 approach for temperature monitoring during breast MR-guided focused ultrasound surgery treatments.** *Magn Reson Med* 2014;72:793–99 CrossRef Medline

41. Peters RD, Henkelman RM. **Proton-resonance frequency shift MR thermometry is affected by changes in the electrical conductivity of tissue.** *Magn Reson Med* 2000;43:62–71 CrossRef Medline

42. Maier SE, Scheidegger MB, Liu K, et al. **Accurate velocity mapping with FAcE.** *Magn Reson Imaging* 1996;14:163–71 CrossRef Medline

43. Greitz D, Wirestam R, Franck A, et al. **Pulsatile brain movement and associated hydrodynamics studied by magnetic resonance phase imaging: the Monro-Kellie doctrine revisited.** *Neuroradiology* 1992;34:370–80 CrossRef Medline

44. Enzmann DR, Pelc NJ. **Brain motion: measurement with phase-contrast MR imaging.** *Radiology* 1992;185:653–60 CrossRef Medline

45. Peters NH, Bartels LW, Sprinkhuizen SM, et al. **Do respiration and cardiac motion induce magnetic field fluctuations in the breast and are there implications for MR thermometry?** *J Magn Reson Imaging* 2009;29:731–35 CrossRef Medline

46. Kim K, Diederich C, Narsinh K, et al. **Motion-robust, multi-slice, real-time MR thermometry for MR-guided thermal therapy in abdominal organs.** *Int J Hyperthermia* 2023;40:2151649 CrossRef Medline

47. Vigen KK, Daniel BL, Pauly JM, et al. **Triggered, navigated, multi-baseline method for proton resonance frequency temperature mapping with respiratory motion.** *Magn Reson Med* 2003;50:1003–10 CrossRef Medline

48. de Senneville BD, Mougenot C, Moonen CTW. **Real-time adaptive methods for treatment of mobile organs by MRI-controlled high-intensity focused ultrasound.** *Magn Reson Med* 2007;57:319–30 CrossRef Medline

49. Grissom WA, Lustig M, Holbrook AB, et al. **Reweighted ℓ1 referenceless PRF shift thermometry.** *Magn Reson Med* 2010;64:1068–77 CrossRef Medline

50. Rieke V, Vigen KK, Sommer G, et al. **Referenceless PRF shift thermometry.** *Magn Reson Med* 2004;51:1223–31 CrossRef Medline

51. Kuroda K, Kokuryo D, Kumamoto E, et al. **Optimization of self-reference thermometry using complex field estimation.** *Magn Reson Med* 2006;56:835–43 CrossRef Medline

52. Grissom WA, Rieke V, Holbrook AB, et al. **Hybrid referenceless and multibaseline subtraction MR thermometry for monitoring thermal therapies in moving organs.** *Med Phys* 2010;37:5014–26 CrossRef Medline

53. Shmatukha AV, Bakker CJG. **Correction of proton resonance frequency shift temperature maps for magnetic field disturbances caused by breathing.** *Phys Med Biol* 2006;51:4689–705 CrossRef Medline

54. Toupin S, Senneville B. D, Ozenne V, et al. **Combination of principal component analysis and optical-flow motion compensation for improved cardiac MR thermometry.** *Phys Med Biol* 2017;62:1208–24 CrossRef Medline

55. Wu M, Mulder HT, Baron P, et al. **Correction of motion-induced susceptibility artifacts and B₀ drift during proton resonance frequency shift-based MR thermometry in the pelvis with background field removal methods.** *Magn Reson Med* 2020;84:2495–511 CrossRef Medline

56. de Senneville BD, Coupé P, Ries M, et al. **Deep correction of breathing-related artifacts in real-time MR-thermometry.** *Comput Med Imaging Graph* 2021;87:101834 CrossRef Medline

57. Parker DL, Payne A, Odéen H. **A k-space-based method to measure and correct for temporal B0 field variations in MR temperature imaging.** *Magn Reson Med* 2022;88:1098–111 CrossRef Medline

58. Pruessmann KP, Weiger M, Scheidegger MB, et al. **SENSE: sensitivity encoding for fast MRI.** *Magn Reson Med* 1999;42:952–62

59. Bitton RR, Sheingaouz E, Assif B, et al. **Evaluation of an MRI receive head coil for use in transcranial MR guided focused ultrasound for functional neurosurgery.** *Int J Hyperthermia* 2021;38:22–29 CrossRef Medline

60. Minalga E, Payne A, Merrill R, et al. **An 11-channel radio frequency phased array coil for magnetic resonance guided high-intensity focused ultrasound of the breast.** *Magn Reson Med* 2013;69:295–302 CrossRef Medline

61. Gaur P, Grissom WA. **Accelerated MRI thermometry by direct estimation of temperature from undersampled k-space data.** *Magn Reson Med* 2015;73:1914–25 CrossRef Medline

62. Fielden SW, Feng X, Zhao L, et al. **A spiral-based volumetric acquisition for MR temperature imaging.** *Magn Reson Med* 2018;79:3122–27 CrossRef Medline

63. Zhang L, Armstrong T, Li X, et al. **A variable flip angle golden-angle-ordered 3D stack-of-radial MRI technique for simultaneous proton resonant frequency shift and T1-based thermometry.** *Magn Reson Med* 2019;82:2062–76 CrossRef Medline

64. Jonathan SV, Grissom WA. **Volumetric MRI thermometry using a three-dimensional stack-of-stars echo-planar imaging pulse sequence.** *Magn Reson Med* 2018;79:2003–13 CrossRef Medline

65. Pauly BK. **Magnetic resonance acoustic radiation force (impulse) imaging (MR-ARFI).** *J Ther Ultrasound* 2015;3:O34 CrossRef

66. Kaye EA, Chen J, Pauly KB. **Rapid MR–ARFI method for focal spot localization during focused ultrasound therapy.** *Magn Reson Med* 2011;65(3):738–743 CrossRef Medline

67. Hectors SJ, Jacobs I, Moonen CTW, et al. **MRI methods for the evaluation of high intensity focused ultrasound tumor treatment: current status and future needs.** *Magn Reson Med* 2016;75:302–17 CrossRef Medline

68. Wijlemans JW, Deckers R, van den Bosch MA, et al. **Evolution of the ablation region after magnetic resonance-guided high-intensity focused ultrasound ablation in a Vx2 tumor model.** *Invest Radiol* 2013;48:381–86 CrossRef Medline

69. Dinger SC, Fridjhon P, Rubin DM. **Thermal excitation of gadolinium-based contrast agents using spin resonance.** *PLoS One* 2016;11: e0158194 CrossRef Medline

70. Morochnik S, Ozhinsky E, Rieke V, et al. **T2 mapping as a predictor of nonperfused volume in MRgFUS treatment of desmoid tumors.** *Int J Hyperthermia* 2019;36:1272–77 CrossRef Medline

71. Hölscher T, Raman R, Fisher DJ, et al. **Effects of varying duty cycle and pulse width on high-intensity focused ultrasound (HIFU)-induced transcranial thrombolysis.** *J Ther Ultrasound* 2013;1:18 CrossRef Medline

72. Huang Y, Lipsman N, Schwartz ML, et al. **Predicting lesion size by accumulated thermal dose in MR-guided focused ultrasound for essential tremor.** *Med Phys* 2018;45:4704–10 CrossRef Medline

73. Hundt W, Yuh EL, Steinbach S, et al. **Effect of continuous high intensity focused ultrasound in a squamous cell carcinoma tumor model compared to muscle tissue evaluated by MRI, histology, and gene expression.** *Technol Cancer Res Treat* 2009;8:85–98 CrossRef Medline

74. Hectors SJ, Jacobs I, Strijkers GJ, et al. **Multiparametric MRI analysis for the identification of high intensity focused ultrasound-treated tumor tissue.** *PLoS One* 2014;9:e99936 CrossRef Medline

75. Le Ster C, Mauconduit F, Mirkes C, et al. **Measuring radiofrequency field-induced temperature variations in brain MRI exams with motion compensated MR thermometry and field monitoring.** *Magn Reson Med* 2022;87:1390–1400 CrossRef Medline